arXiv:1301.3540v1 [cond-mat.str-el] 16 Jan 2013

Ground State of Electrons in Bilayer Graphene

Xin-Zhong Yan[1] and C. S. Ting[2]
[1] *Institute of Physics, Chinese Academy of Sciences, P.O. Box 603, Beijing 100190, China*
[2] *Texas Center for Superconductivity, University of Houston, Houston, Texas 77204, USA*

(Dated: January 17, 2013)

Based on the four-band continuum model, we study the petaloid-loop-current (PLC) state for electrons in bilayer graphene at the charge neutrality point. The present work resolves the puzzles that (a) the energy gap increases significantly with increasing the magnetic field B, (b) the energy gap can be closed by the external electric field of either polarization, and (c) the particle-hole spectrum is asymmetric in the presence of B, all these as observed by the experiment. We also present the prediction of the hysteresis energy gap behavior with varying B, which explains the existing experimental observation on the electric conductance at weak B. The large energy gap of the PLC state is shown to originate from the disappearance of Landau levels of $n = 0$ and 1 states in conduction band. By comparing with the existing models and the experiments, we conclude that the PLC state is a possible ground state of electrons in bilayer graphene.

PACS numbers: 73.22.Pr,71.70.Di,71.10.-w,71.27.+a

The study of bilayer graphene (BLG) is a focused area in the condensed-matter physics because of the potential application of BLG to new electronic devices [1–4]. One of the fundamental subjects is to explore the physics of the ground state of electrons in BLG. A number of experiments [5–8] performed on high quality suspended BLG samples have provided the evidence that the ground state is gapped at the charge neutrality point. In particular, a recent experiment by Velasco *et al.* [7] has observed that (i) the ground state is insulating in the absence of external electric and magnetic fields, with a gap $E_{\rm gap} \approx 2$ meV that can be closed by a perpendicular electric field of either polarization; (ii) the gap grows with increasing magnetic field B as $E_{\rm gap} = \Delta_0 + \sqrt{a^2B^2 + \Delta_0^2}$ with $\Delta_0 \approx 1$ meV and $a \approx 5.5$ meVT^{-1}; and (iii) the state is particle-hole asymmetric. On the other hand, theories have predicted various gapped states, such as a ferroelectric-layer asymmetric state [9–13] or quantum valley Hall state (QVH) [14], a layer-polarized antiferromagnetic state (AF) [15], a quantum anomalous Hall state (QAH) [12, 16, 17], a quantum spin Hall state (QSH) [12, 17], and a superconducting state in coexistence with antiferromagnetism (SAF) [18]. The ferroelectric-layer asymmetric and QAH and QSH states all have been ruled out by the experiment [7]. The SAF state is excluded because the real system is insulator. The AF state cannot reproduce the gap behavior with varying the magnetic field. A candidate proposed very recently is the loop-current state that is a broken inversion and time-reversal symmetry state [19, 20]. This state has been studied by numerical diagonalization of an effective mean-field Hamiltonian for a finite size lattice in presence of the magnetic field [19] and by analytical solving a two-band continuum model (2BCM) [20]. By viewing the structure of the current loops connected to each lattice site [20], we here name it as the petaloid-loop current (PLC) state. Whether the model of PLC state agrees with the experimental observations on the electronic properties of BLG remains a question.

In this work, using the four-band continuum model (4BCM) for electrons with finite-range repulsive interactions in BLG, we study the PLC state at the charge neutrality point and compare the results with the experimental observations. We investigate the gap behavior of the PLC state with varying the magnetic field B, and the particle-hole asymmetry spectra at finite B, and the phase transitions in the electron system in the presence of the electric and magnetic fields. We will show that the puzzles (i)-(iii) of the experimental observations can be resolved by the present model.

The 4BCM. The top view of the lattice structure of a BLG is shown in Fig. 1(a). The unit cell of BLG contains four atoms denoted as a$_1$ and b$_1$ on top layer, and a$_2$ and b$_2$ on bottom layer. The lattice constant defined as the distance between the nearest-neighbor (NN) atoms of a sublattice is $a \approx 2.4$ Å . The distance between the two layers is $d \approx 3.34$ Å . The energy of intralayer NN [between a$_1$ (a$_2$) and b$_1$ (b$_2$)] and interlayer NN (between b$_1$ and a$_2$) electron hopping are $t \approx 2.8$ eV and $t_1 \approx 0.39$ eV, respectively. The reciprocal lattice of a single layer and the first Brillouin zone are shown in Fig. 1(b).

For the carrier concentration close to the charge neutrality point, we need to consider only the states close to the zero energy. Since the momenta of the low-energy states are close to the Dirac points $K = (4\pi/3, 0)$ and $K' = -K$, we here define the operator

$$C^\dagger_{vk\sigma} = (c^\dagger_{a_1,v+k,\sigma}, c^\dagger_{b_1,v+k,\sigma}, c^\dagger_{a_2,v+k,\sigma}, c^\dagger_{b_2,v+k,\sigma})$$

where $v = K$ or K', $c^\dagger_{l,v+k,\sigma}$ creates a spin-σ electron of momentum k in valley v of l sublattice, and k is measured from the Dirac point K (K') and confined to a circle $k \le 1/a$ of K (K') valley as shown in Fig. 1(b). In the momentum space, the Hamiltonian describing the

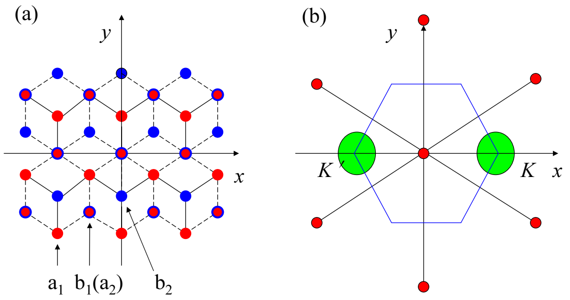

FIG. 1: (Color online) (a) Top view of the bilayer graphene. Atoms a$_1$ (a$_2$) and b$_1$ (b$_2$) are on the top (bottom) layer. (b) The first Brillouin zone (hexagon) and the two valleys K and K' in the reciprocal-lattice space of honeycomb lattice.

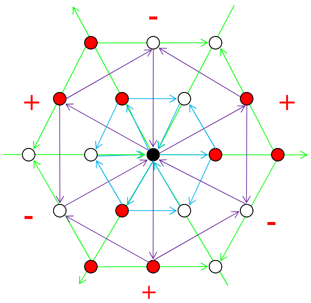

FIG. 2: (Color online) Some of the current loops connected to the black site on a sublattice. The sign factor ± in $I_{ll}(\vec{j}-\vec{i}) \equiv \pm J_l(|\vec{j}-\vec{i}|)$ is + (-) for the electron motion from the black site i to the red (white) site j.

noninteracting electrons is given by

$$H_0 = \sum_{vk\sigma} C^\dagger_{vk\sigma} H^0_{vk} C_{vk\sigma} \tag{1}$$

and

$$H^0_{vk} = \begin{pmatrix} 0 & e_{vk} & 0 & 0 \\ e^*_{vk} & 0 & -t_1 & 0 \\ 0 & -t_1 & 0 & e_{vk} \\ 0 & 0 & e^*_{vk} & 0 \end{pmatrix} \tag{2}$$

where $e_{vk} = \epsilon_0(s_v k_x + i k_y)$, $s_v = 1$ (-1) for k in the valley K (K'), and $\epsilon_0 = \sqrt{3}t/2$. We hereafter use the units of $\epsilon_0 = 1$ and $a = 1$.

The interaction Hamiltonian is given as

$$H' = U \sum_{lj} \delta n_{lj\uparrow} \delta n_{lj\downarrow} + \frac{1}{2} \sum_{li \neq l'j} v_{li,l'j} \delta n_{li} \delta n_{l'j} \tag{3}$$

where $\delta n_{li\sigma}$ is the number deviation of electrons with spin σ from its average occupation at site i of sublattice l (hereafter denoted as li for short), $\delta n_{li} = \delta n_{li\uparrow} + \delta n_{li\downarrow}$, U is the on-site interaction, and $v_{li,l'j}$ is the interaction between electrons at sites li and $l'j$. Within the mean-field approximation (MFA), since the interaction $v_{li,l'j}$ appears in the exchange self-energy, it can be considered as a finite-range interaction by taking into account the screening effect due to the electronic charge fluctuations [21]. The total Hamiltonian $H_0 + H'$ satisfies the particle-hole symmetry [21].

The PLC state. Under the MFA, the self-energy $\Sigma_{ll'}(k)$ of electrons in the PLC state is obtained as

$$\Sigma_{ll'}(k) = \sum_{\vec{d} \neq 0} v_{li,l'j} \langle c_{li\sigma} c^\dagger_{l'j\sigma} \rangle \exp(i\vec{k} \cdot \vec{d}) \tag{4}$$

with $\langle c_{li\sigma} c^\dagger_{l'j\sigma} \rangle = R_{ll'}(d) + i I_{ll'}(\vec{d})$, where $\vec{d}$ is a vector from the position li to $l'j$. The quantity $I_{ll'}(\vec{d})$ is proportional to a current. First, we consider the diagonal self-energy $\Sigma_{ll}(k)$ for the same sublattice l. The formulae for $R_{ll}(d)$ and $I_{ll}(\vec{d})$ are derived in the supplement. As mentioned above, only the low-energy states with momenta close to the Dirac points need to be considered. Then by expanding the self-energy with respect to k in the two valleys and taking only the leading terms $\Sigma_{ll}(\pm K)$, we obtain (see the supplement)

$$\begin{aligned} \Sigma_{ll}(\pm K) &= r_l v_c \pm d_l v_s \\ r_l &= \frac{1}{N} \sum_k \left(1 - \left\langle c^\dagger_{lK'+k\sigma} c_{lK'+k\sigma} \right\rangle - \left\langle c^\dagger_{lK+k\sigma} c_{lK+k\sigma} \right\rangle \right) \\ d_l &= \frac{1}{N} \sum_k \left(\left\langle c^\dagger_{lK'+k\sigma} c_{lK'+k\sigma} \right\rangle - \left\langle c^\dagger_{lK+k\sigma} c_{lK+k\sigma} \right\rangle \right) \\ v_c &= \sum_{\vec{d} \neq 0} v(d) \cos^2(\vec{K} \cdot \vec{d}) \\ v_s &= \sum_{\vec{d} \neq 0} v(d) \sin^2(\vec{K} \cdot \vec{d}) \end{aligned} \tag{5}$$

where r_l and d_l come respectively from the parts $R_{ll}(d)$ and $I_{ll}(\vec{d})$, the k summations here are confined to a single valley, $v(d) = v_{li,lj}$, and N is the total number of unit cells on single layer graphene. The quantity r_l can be written as $r_l = -\delta_l/2$ with δ_l as the average electron doping concentration on sublattice l. For the homogeneous system at the charge neutrality point, we have $r_l = 0$. The quantity $d_l v_s$ is the order parameter of the PLC state. In Fig. 2, we draw out all of the current loops on the same sublattice connected to a given site i. Clearly, the total current density at site i is zero. The existence of the current loops breaks the time-reversal symmetry.

Second, when the quantity $I_{ll'}(\vec{d})$ with $l \neq l'$ is not vanishing, it breaks the translational invariance of the system. This case happens only when the interactions are strong enough. For weak to medium interactions, we here assume all the currents between the bonds of different sublattices are negligible small (see the supplement and Ref. 19).

A particular property of the PLC state is that the order parameter term is odd for interchanging the valley index. We suppose $d_{a_1}v_s = -d_{b_2}v_s \equiv -\Delta_1$ and $d_{b_1}v_s = -d_{a_2}v_s \equiv \Delta_2$ that means the breaking of the layer inversion symmetry. As a result, the effective MFA Hamiltonian H_{vk} is obtained by adding the diagonal matrix $\mathrm{Diag}(-s_v\Delta_1, s_v\Delta_2, -s_v\Delta_2, s_v\Delta_1)$ to H^0_{vk}. Note that the matrices H_{vk} and H_{-vk} are related by $H_{vk} = SH_{-v-k}S$, where S is a 4×4 matrix with elements $S_{\mu\nu} = \delta_{\mu,5-\nu}$. If ψ^μ_k is an eigenfunction of H_{vk} with eigenvalue E^μ_k (μ = 1,2,3,4), then $S\psi^\mu_k$ is an eigenfunction of H_{-v-k} with the same eigenvalue. Therefore, only the eigenstates in a single valley need to be solved, which give rise to the whole energy spectra.

1. The PLC state at B = 0. With the wave functions, the order parameters are determined by

$$\Delta_1 = \frac{\sqrt{3}v_s}{2V}\sum_{k\mu}{}' f(E^\mu_k)(|\psi^{1\mu}_k|^2 - |\psi^{4\mu}_k|^2) \qquad (6)$$

$$\Delta_2 = \frac{\sqrt{3}v_s}{2V}\sum_{k\mu}{}' f(E^\mu_k)(|\psi^{3\mu}_k|^2 - |\psi^{2\mu}_k|^2) \qquad (7)$$

where f is the Fermi distribution function, $\psi^{\nu\mu}_k$ is the νth component of the eigenfunction ψ^μ_k, $V = \sqrt{3}N/2$ is the total area of the one layer lattice, and the k summation runs over a single valley. From the 2BCM, we know that the valence and conduction bands are connected to the electronic motions in the a$_1$ and b$_2$ sublattices. Therefore, the energy gap between the valence and conduction bands is determined by $2\Delta_1$. To reproduce the experimental data $|\Delta_1| = 1$ meV at the charge neutrality point, v_s needs to be $5.8\epsilon_0$. Supposing the effective interaction $v(r) \approx e^2\exp(-q_0 r)/r\epsilon$ with $\epsilon \approx 3$ as the screening constant of high frequency limit of BLG, we can obtain the desired value v_s with $q_0 \approx 4.54/a$. Another coupling constant is obtained as $v_c \approx 1.94\epsilon_0$.

2. The PLC state at finite B. In the presence of the magnetic field B applied perpendicularly to the sample plane, we take the Landau gauge for the vector potential, $\vec{A} = (0, Bx)$. With this gauge, the y component momentum k_y is a good quantum number. Replacing the variable x and the operator $k_x = -i\nabla_x$ with the raising and lowering operators $a^\dagger$ and a, $k_y + Bx = \sqrt{B/2}(a^\dagger + a)$ and $k_x = i\sqrt{B/2}(a^\dagger - a)$, we can rewrite the effective Hamiltonian in real space. The eigenfunction $\psi^\mu_{Kn}(j)$ (with μ = 1,2,3,4) can be expressed as

$$\psi^\mu_{Kn}(j) = \begin{pmatrix} ix^{1\mu}_{Kn}\phi_n(j) \\ x^{2\mu}_{Kn}\phi_{n-1}(j) \\ x^{3\mu}_{Kn}\phi_{n-1}(j) \\ -ix^{4\mu}_{Kn}\phi_{n-2}(j) \end{pmatrix} \qquad (8)$$

for $n \geq 2$, where $\phi_n(j)$ is the nth level wave function of a harmonic oscillator of frequency $2B$ and mass 1/2 centered at $x_c = -k_y/B$. The vector $X^\mu_{Kn} = (x^{1\mu}_{Kn}, x^{2\mu}_{Kn}, x^{3\mu}_{Kn}, x^{4\mu}_{Kn})^t$ (with the superscript t meaning the transpose of the vector) and the eigenenergy E^μ_{Kn} are determined by

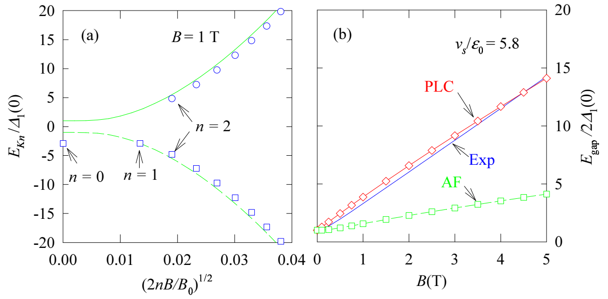

FIG. 3: (Color online) (a) Landau levels E^μ_{Kn} in the valence (squares) and conduction (circles) bands at $B = 1$ T. The solid and dashed lines represent continuum conduction and valence energy bands, respectively, at $B = 0$ with the abscissa being momentum k. (b) The energy gap $E_{\rm gap}$ (diamonds) as function of the magnetic field B compared with the AF result and the experimental observation (Exp, Ref. 7).

$$H_{Kn}X^\mu_{Kn} = E^\mu_{Kn}X^\mu_{Kn} \qquad (9)$$

with

$$H_{Kn} = \begin{pmatrix} -\Delta_1 & \sqrt{2Bn} & 0 & 0 \\ \sqrt{2Bn} & \Delta_2 & -t_1 & 0 \\ 0 & -t_1 & -\Delta_2 & \sqrt{2B(n-1)} \\ 0 & 0 & \sqrt{2B(n-1)} & \Delta_1 \end{pmatrix}.$$

The vector X^μ_{Kn} is normalized to unity. For each $n \geq 2$, the four energy levels appear at the valence, conduction, and other two bands about $\pm t_1$ far from the zero energy, respectively. For $n = 1$, there are only three states with $x^{4\mu}_{K1} = 0$ and the other three components and eigenvalues are determined by the upper left 3×3 matrix of H_{K1}. For $n = 0$, we have only one state $X^{1t}_{K0} = (1, 0, 0, 0)$ and $E^1_{K0} = -\Delta_1$. To self-consistently determine the order parameters, we need to calculate the quantity d_l. The k summation in Eq. (5) now is changed to the sum over the quasiparticle states. The order parameters are now determined by

$$\Delta_1 = \frac{\sqrt{3}v_s B}{4\pi}\sum_{n\mu} f(E^\mu_{Kn})[|x^{1\mu}_{Kn}|^2 - |x^{4\mu}_{Kn}|^2], \qquad (10)$$

$$\Delta_2 = \frac{\sqrt{3}v_s B}{4\pi}\sum_{n\mu} f(E^\mu_{Kn})[|x^{3\mu}_{Kn}|^2 - |x^{2\mu}_{Kn}|^2]. \qquad (11)$$

Here $B/2\pi$ is the degeneracy of a Landau level, and B is in the unit of $B_0 = \hbar c/ea^2 = 1.105\times 10^4$T.

The solution to the Landau levels at $B = 1$ T is shown in Fig. 3(a). Only the levels in the conduction and valence bands are depicted. For $n = 0$ there is only one state of energy $-\Delta_1(B)$ in the valence band. For $n = 1$,

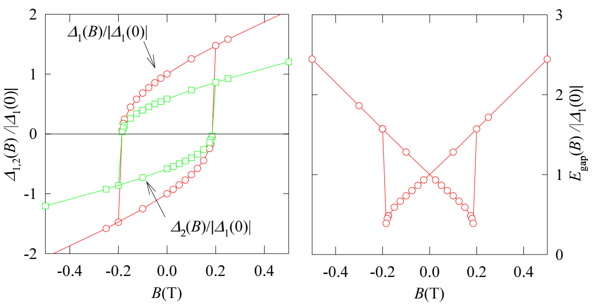

FIG. 4: (Color online) The hysteresis curves for $\Delta_1(B)$, $\Delta_2(B)$ (left) and $E_{\rm gap}(B)\Delta_1(0)$ (right).

there is a level E^v_{K1} slightly above $-\Delta_1(B)$ in the valence band. There is no state in the conduction band for $n = 0$ and 1. Only when $n \geq 2$, the level E^c_{Kn} in the conduction band appears. The energy gap is

$$E_{\rm gap} = E^c_{K2} - E^v_{K1}. \tag{12}$$

Clearly, the particle-hole symmetry is no longer valid at finite B, in agreement with the experiment [7]. Fig. 3(b) shows the energy gap $E_{\rm gap}$ of the PLC state as function of the magnetic field B. The AF calculation of the same 4BCM and experimental results for $E_{\rm gap}$ are also plotted for comparison. Here, the only fitting parameter is v_s for reproducing $\Delta_1(0) = \Delta_0$ at $B = 0$. The theoretical result for $E_{\rm gap}$ of the PLC state as a function of B is in surprisingly good agreement with the experiment [7].

The above solution to the order parameters is only in the branch of $\Delta_1 > 0$ and $\Delta_2 > 0$. At weak magnetic field $B > 0$, there is another branch in which $\Delta_1 < 0$ and $\Delta_2 < 0$. In this case, the two levels of $n = 0$ and 1 appear in the conduction band but not in valence the band, and the energy band is given by $E_{\rm gap} = E^c_{K1} - E^v_{K2}$. In Fig. 4, we show the hysteresis curves for the PLC order parameters $\Delta_1(B)$ and $\Delta_2(B)$ and the energy gap $E_{\rm gap}$ in the range -0.5 T $< B <$ 0.5 T. For $|B| \leq 0.18$ T, there are two branches for $E_{\rm gap}$. In the lower gap branch, the gap decreases with increasing $|B|$. This behavior of $E_{\rm gap}$ is in qualitative agreement with the experiment observation by Weitz et al. [5] that indicates two peaks in the electric conductance appearing at $B_p \approx \pm 0.04$ T (where the real gap reaches the minimum), respectively.

The AF state. In the AF state, the two layers have opposite magnetizations that stem from the on-site interaction U. We denote the magnetizations in a unit cell as $(m_{a_1}, m_{b_1}, m_{a_2}, m_{b_2})$. The order parameters are given by $-U(m_{a_1}, m_{b_1}, m_{a_2}, m_{b_2}) \equiv (-\Delta_1, \Delta_2, -\Delta_2, \Delta_1)$.

At $B = 0$, the equations for determining the order parameters happen to be the same as Eqs. (6) and (7). To reproducing the energy gap of the experimental data, $U = v_s \approx 5.8\epsilon_0$ is needed. (See supplement.)

At finite B, the spectra of the electrons are different from the PLC state. At valley K, the Landau levels have the similar distribution as the PLC state. In particular, there are no levels of $n = 0$ and 1 in the conduction (valence) band if $\Delta_1 > (<) 0$. However, at valley K', these levels appear but their counterparts disappear in the valence (conduction) band. As a result, the energy gap is not as large as the PLC state but is $2\Delta_1(B)$. The self-consistent solution for the energy gap in the presence of B is shown in Fig. 3(b). Obviously, the B-dependent AF gap cannot explain the experimental result.

The PLC state under external electric field. When an external electric field E is applied perpendicularly to the BLG plane, there is a potential difference $2u = Eed/\epsilon$ between the two layers. The Hamiltonian H_{vk} now is obtained by adding the diagonal matrix Diag$(u + r_1 v_c - s_v\Delta_1, u + r_2 v_c + s_v\Delta_2, -u - r_2 v_c - s_v\Delta_2, -u - r_1 v_c + s_v\Delta_1)$ to H^0_{vk}. Here the terms $r_l v_c$ appear because of the electric polarization by E. Note that r_l has the same sign of u, and thereby $H_{vk}(u) = SH_{-v-k}(-u)S$, which means that the order parameters are even functions of u. The model shows that if an external electric field in positive direction closes the energy gap, then an electric field in negative direction does it either. For the sake of illustration, we here consider the case of $B \geq 0$ and $u > 0$. The results for other cases can be deduced by the symmetry of the Hamiltonian. For $B \geq 0$ and $u > 0$, we still have two cases: $\Delta_1 > 0$ and $\Delta_1 < 0$. Here, we consider the case of $\Delta_1 > 0$. The discussion can be extended to the case of $\Delta_1 < 0$. At $B = 0$, the effective gap is $u + r_1 v_c - \Delta_1$. The critical potential u_0 closing the effective gap is obtained as $u_0 \approx 0.48\Delta_0 \approx 0.48$ meV. The critical field of the experimental data [7] is $E \approx 1.25$ mVÅ^{-1}, which corresponds to $u_0 \approx 0.69$ meV (using $\epsilon \approx 3$). The theory is in qualitative agreement with the experiment.

Since the system satisfies the particle-hole symmetry at $B = 0$, we can take the chemical potential as zero for the system at the charge neutrality point. Then, the level $u + r_1 v_c - \Delta_1$ is occupied if its sign is negative, otherwise it is empty. Therefore, with increasing u from 0, the system undergoes a phase transition at $u = u_0$ from the state with the level $u + r_1 v_c - \Delta_1$ occupied to the state with the level empty. Thus, to search the critical u_0 where the gap closes at finite B, we study the phase transition.

At finite B, a state at (B, u) can be obtained by continuously changing the parameters B and u from the state at $(0, u_i)$. If $u_i > u_0(0)$, then the level $u + r_1 v_c - \Delta_1$ is empty. Note that $u + r_1 v_c - \Delta_1$ is the only Landau level E_{Kn} of $n = 0$ at finite B and there is another level of $n = 1$ close to it similarly as the case of $u = 0$. So the two levels of $n = 0$ and 1 in the K valley keep empty on the path from $(0, u_i)$ to (B, u). On the other hand, if one starts from an initial state with $u_i < u_0(0)$, then the two levels of $n = 0$ and 1 keep filled. (We denote the filling number as $f_K = 0$ and 1 for the two levels empty and filled, respectively.) We thus have two states at (B, u). To judge which one is the real ground state,

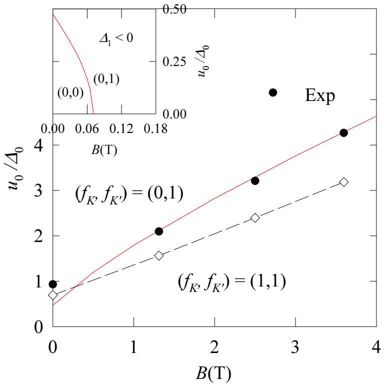

FIG. 5: (Color online) Phase boundary $u_0(B)$ between the two phases $(f_K, f_{K'}) = (0,1)$ and $(1,1)$ (red solid line). The solid points and the diamonds are converted from the critical E of the experimental data (Ref. 7) using $\epsilon \approx 2.24$ and 3, respectively. The inset shows the result for $\Delta_1 < 0$ in the range $0 < B < 0.18$ T.

we compare their ground-state energies. With the energy judgment, the ground state at (B, u) is uniquely determined. At the critical potential $u_0(B)$, the two states have the same ground-state energy.

In Fig. 5, we exhibit the result for $u_0(B)$ as function of B and compare it with the experimental data [7]. The experimental data are obtained by converting the critical electric field E to u_0 according to $u_0 = Eed/2\epsilon$ with the dielectric constant $\epsilon \approx 2.24$ (solid points) and 3 (diamonds). As seen from Fig. 5, the behavior of $u_0(B)$ by the theoretical calculation is in fairly good agreement with the experiment [7] with $\epsilon \approx 2.24$.

As already seen, there is another solution of $\Delta_1 < 0$ in the range $0 < B < 0.18$ T. We show in the insert in Fig. 5 the phase boundary for this case. We see that the state of $\Delta_1 < 0$ in $0.07 < B < 0.18$ T is unstable with respect to a small E. The range for the stable state of $\Delta_1 < 0$ is reduced to $|B| < 0.07$ T, with $|B_{max}| = 0.07$ T close toward to the experimental data [5] $|B_p| = 0.04$ T.

Summary. With the MFA to the 4BCM, we have studied the PLC state of the electrons with finite-range repulsive interactions in BLG at the charge neutrality point. Because of the broken inversion and time-reversal symmetry in the PLC state, the Landau levels of $n = 0$ and 1 states in the conduction/valence band disappear. With only one coupling constant v_s fitting the experimental gap Δ_0 at $B = 0$, the obtained energy gap at finite B is in surprisingly good agreement with experimental data [7]. The results for the phase transition in the system in the presence of external electric and magnetic fields, and the particle-hole asymmetry spectra in the presence of B are also in good agreements with the experimental observations [7]. There is also the intermediate experimental support [5] for the prediction for the hysteresis energy gap behavior with varying B. These facts show that the PLC state is a possible ground state of electrons in BLG. The model explored here can be useful for understanding the physics of the electrons in BLG that is expected as a new generation of semiconductor.

This work was supported by the National Basic Research 973 Program of China under Grants No. 2011CB932702 and No. 2012CB932302, NSFC under Grant No. 10834011, and the Robert A. Welch Foundation under Grant No. E-1146.

[1] T. Ohta, A. Bostwick, T. Seyller, K. Horn, E. Rotenberg, Science **313**, 951 (2006).
[2] J. B. Oostinga, H. B. Heersche, X. Liu, A. F. Morpurgo, and L. M. K. Vanderspen, Nature Mater. **7**, 151 (2008).
[3] E. McCann, Phys. Rev. B **74**, 161403(R) (2006).
[4] E. V. Castro, K. S. Novoselov, S. V. Morozov, N. M. R. Peres, J. M. B. Lopes dos Santos, J. Nilsson, F. Guinea, A. K. Geim, and A. H. Castro Neto, Phys. Rev. Lett. **99**, 216802 (2007).
[5] R. T. Weitz, M. T. Allen, B. E. Feldman, J. Martin, and A. Yacoby, Science **330**, 812 (2010).
[6] F. Freitag, J. Trbociv, M. Weiss, and C. Schn̈enberger, Phys. Rev. Lett. **108**, 076602 (2012).
[7] J. Velasco Jr., L. Jing, W. Bao, Y. Lee, P. Kratz, V. Aji, M. Bockrath, C. N. Lau, C. Varma, R. Stillwell, D. Smirnov, F. Zhang, J. Jung, and A. H. MacDonald, Nature Nanotech. **7**, 156 (2012).
[8] W. Bao, J. Velasco Jr., L. Jing, F. Zhang, B. Standley, D. Smirnov, M. Bockrath A. H. MacDonald, and C. N. Lau, Proc. Natl. Acad. Sci. USA **109**, 10802 (2012).
[9] H. K. Min, G. Borghi, M. Polini, and A. H. MacDonald, Phys. Rev. B **77**, 041407(R) (2008).
[10] R. Nandkishore and L. Levitov, Phys. Rev. Lett. **104**, 156803 (2010).
[11] F. Zhang, H. K. Min, M. Polini, and A. H. MacDonald, Phys. Rev. B **81**, 041402(R) (2010).
[12] J. Jung, F. Zhang, and A. H. MacDonald, Phys. Rev. B **83**, 115408 (2011).
[13] A. H. MacDonald, J. Jung, and F. Zhang, Phys. Scr. **T146**, 014012 (2012).
[14] F. Zhang and A. H. MacDonald, Phys. Rev. Lett. **108**, 186804 (2012).
[15] E. V. Gorbar, V. P. Gusynin, V. A. Miransky, and I. A. Shovkovy, Phys. Rev. B **85**, 235460 (2012).
[16] R. Nandkishore and L. Levitov, Phys. Rev. B **82**, 115124 (2010).
[17] F. Zhang, J. Jung, G. A. Fiete, Q. Niu, and A. H. MacDonald, Phys. Rev. Lett. **106**, 156801 (2011).
[18] M.V. Milovanović and S. Predin, Phys. Rev. B **86**, 195113 (2012).
[19] L. J. Zhu, V. Aji, and C. M. Varma, arXiv: 1202.0821.
[20] X.-Z. Yan and C. S. Ting, Phys. Rev. B 86, 235126 (2012).
[21] X.-Z. Yan and C. S. Ting, Phys. Rev. B **86**, 125438 (2012).